DOI: 10.1002/adfm.200600257

Siloxane Copolymers for Nanoimprint Lithography**

By *Philip Choi*, *Peng-Fei Fu*,* and *L. Jay Guo**

Presented here is the novel use of thermoplastic siloxane copolymers as nanoimprint lithography (NIL) resists for 60 nm features. Two of the most critical steps of NIL are mold release and pattern transfer through dry etching. These require that the NIL resist have low surface energy and excellent dry-etching resistance. Homopolymers traditionally used in NIL, such as polystyrene (PS) or poly(methyl methacrylate) (PMMA), generally cannot satisfy all these requirements as they exhibit polymer fracture and delamination during mold release and have poor etch resistance. A number of siloxane copolymers have been investigated for use as NIL resists, including poly(dimethylsiloxane)-*block*-polystyrene (PDMS-*b*-PS), poly(dimethylsiloxane)-*graft*-poly(methyl acrylate)-*co*-poly(isobornyl acrylate) (PDMS-*g*-PMA-*co*-PIA), and PDMS-*g*-PMMA. The presence of PDMS imparts the materials with many properties that are favorable for NIL, including low surface energy for easy mold release and high silicon content for chemical-etch resistance—in particular, extremely low etch rates (comparable to PDMS) in oxygen plasma, to which organic polymers are quite susceptible. These properties give improved NIL results.

1. Introduction

Nanoimprint lithography (NIL)[1–4] is a fabrication technology that offers high-throughput, ultrahigh resolution patterning at great cost savings compared to most competing next-generation radiative lithography methods. As a result of its rapid development in the past decade and its potential for sub-100 nm lithography, NIL has been listed by MIT's Technology Review as one of ten emerging technologies that are likely to change the world,[5] and the International Technology Roadmap for Semiconductors also recently announced the inclusion of NIL onto their roadmap as a candidate technology to begin in production in 2013.

Two of the most critical steps in NIL are mold release and pattern transfer by dry etching. In this process, patterned relief features are physically molded into a thin layer of polymer resist on the substrate workpiece. Figure 1 illustrates the thermal nanoimprint process, in which the mold and substrate are pressed together with sufficient force and temperature to cause the resist to conform to the patterns. The temperature is reduced back down below the resist's glass-transition temperature (T_g) and the two pieces are separated, leaving the patterned resist on the substrate. The large contact area between the mold and the resist gives rise to good adhesion forces. Ideal mold release should maintain resist shape integrity, and complete mold-resist separation, while the resist remains attached to the substrate. Furthermore, in order for the patterned resist structures to facilitate further lithography, the polymer must possess some chemical-etch selectivity so that it may serve as a masking layer. Up until now, researchers have commonly used commercial thermal plastic materials, such as poly(methyl methacrylate) (PMMA) and polystyrene (PS) as NIL resists. However, these materials are not at all optimized for the special requirements of the NIL process. Selection of a polymer system for use as the NIL resist should consider critical aspects of correct pattern replication, modest imprint temperature and pressure, proper mold release, and etch selectivity.

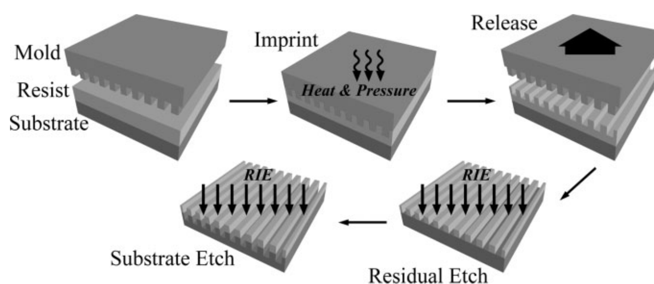

Figure 1. NIL process overview (RIE: reactive ion etching).

Candidate polymers used in imprinting-based lithography should provide reliable releasing properties during the demolding process, while at the same time not compromising their adhesion to the substrate. Commercially available polymer materials such as PMMA are susceptible to mold sticking and fracture defects during mold release that are intolerable for

[*] Prof. L. J. Guo, P. Choi
Department of Electrical Engineering and Computer Science
University of Michigan
Ann Arbor, MI 48109 (USA)
E-mail: guo@eecs.umich.edu
Dr. P.-F. Fu
Dow Corning Corporation
Midland, MI 48686 (USA)
E-mail: pengfei.fu@dowcorning.com

[**] This work was supported by the National Science Foundation (ECS 0424204 and ECS 0508252). The authors thank Dr. Jin-Sung Kim for helping with mold fabrication.

© 2007 WILEY-VCH Verlag GmbH & Co. KGaA, Weinheim

WILEY InterScience DISCOVER SOMETHING GREAT

many device applications.[6,7] During NIL, the large surface-area features of the mold are brought into physical contact with the resist surface, and then separated with a normal force sufficient to overcome the adhesion forces between the mold and resist surfaces. In this respect, the polymer should satisfy these seemingly contradictory requirements of having a low surface energy and high fracture strength, yet maintaining sufficient adhesion to the substrate. Although the mold surface is normally treated with low-surface-energy surfactants[8] when imprinting high-density or high-aspect-ratio patterns, the imprinted polymer still tends to adhere to the mold. Additionally, a polymer with good dry-etching resistance is highly desirable since it can be used directly as a hard mask in reactive-ion-etching (RIE) processes to transfer the patterns into the underlying substrate.

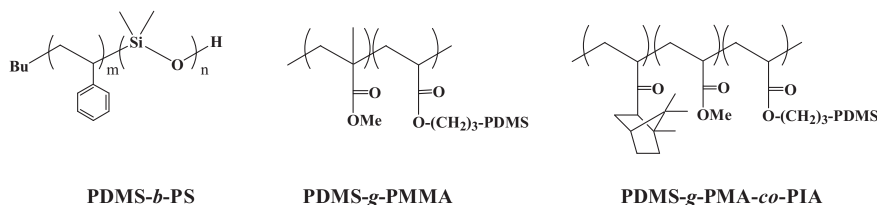

Figure 2. Structures of PDMS-containing copolymers.

To address these critical needs, materials that possess dual surface properties are needed. Of special interest are the poly(dimethylsiloxane) (PDMS)–organic block or graft copolymers.[9–12] In contrast to PMMA and organic polymers in general, siloxane copolymers exhibit significant differences by virtue of the highly open, flexible, and mobile Si–O–Si backbone. These qualities include low surface energy, low T_g, and high thermal stability. Furthermore, it is known that these copolymers undergo microphase segregation above their T_g; this is due to the unfavorable enthalpy of mixing. When cast or hot-pressed on a high-surface-energy substrate such as silicon, glass, or aluminum, the copolymer film forms a lower-surface-energy component (PDMS) enriched air/polymer interface, and a higher-surface-energy component (organic block) dominated polymer/substrate interface.[13–15] The reported dual surface character makes these copolymers excellent candidate materials for NIL; they allow easy mold–resist separation (a lower surface energy) and at the same time good adhesion to the substrate (a higher energy surface). This duality is not possible with homopolymers.

Siloxane copolymers offer another advantage over homopolymers as an NIL resist in that they can offer much improved etching resistance. When exposed to oxygen plasmas, silicon contained in a resist oxidizes, drastically slowing down the etch rate of the polymer.[16] This is in stark contrast to organic polymers, notably PMMA,[17] and bilayer lithography is a common utilization of such material systems.[18]

Compositions investigated in this work include a PDMS-*b*-PS diblock copolymer, PDMS-*g*-PMMA, and PDMS-*g*-PMA-*co*-PIA (PMA: poly(methyl acrylate), PIA: poly(isobornyl acrylate); see Figure 2). This work will explore the novel applicability of these materials to the NIL process in comparison to a PMMA homopolymer. Significant improvements in imprinting large-area samples and dry-etching resistance have been demonstrated. Coating, printing, and etching of the new polymers will be discussed, with particular attention to the critical-performance issues covered in this introduction.

2. Results and Discussion

Resolution capabilities of the PDMS copolymer resist systems can be seen in Figure 3. The smallest feature size on the mold used in this study is 60 nm lines. The mold used to imprint is shown in Figure 3A, which has 60 nm trenches at a 225 nm pitch in a silicon nitride layer on a silicon substrate. Figure 3B–D shows the 72 nm features obtained in various siloxane copolymer resists. The dimensional discrepancy is due to some physical expansion of the resist structures after printing. The mold was vapor-coated with a perfluorinated monolayer to lower its surface energy.[8] The vapor-coating method followed by a thorough anneal produced a stable surfactant coating that did not require any maintenance beyond solvent cleaning during all imprinting tests.

The cross-sectional scans shown in Figure 3B–D are of PDMS-*g*-PMA-*co*-PIA, PDMS-*g*-PMMA, and PS-*b*-PDMS copolymers. The copolymers were dissolved in propylene glycol methyl ether acetate (PGMEA) and spin-coated onto clean silicon wafer substrates. It was found that 4 wt % polymer in solution produced approximately 100 nm for each resist. After coating, the samples were thoroughly baked to remove any residual solvent, to prevent out-gassing during imprinting. Samples were then imprinted at 170 °C and 600 psi for 5 min (100 psi = 689.5 kPa). These imprint parameters are not restrictive, however; a sample of PDMS-*g*-PMA-*co*-PIA resist that was imprinted at 170 °C and 200 psi for 30 s is shown in Figure 3E. Processing parameters can be tailored to specific imprint feature sizes and aspect ratios. Although 60 nm features were the smallest available mold, it is reasonable to say that these resists can be patterned to even finer dimensions. Noticeably, the corner morphology of the graft silicone copoly-

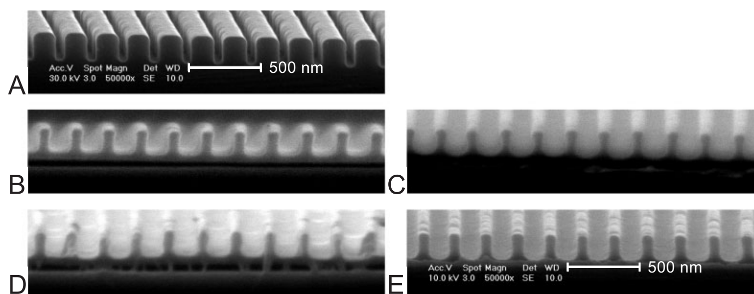

Figure 3. A) The 60 nm feature mold used to imprint into B–D) PDMS-*g*-PMA-*co*-PIA, PDMS-*g*-PMMA, and PS-*b*-PDMS copolymers, respectively. E) PDMS-*g*-PMA-*co*-PIA imprinted at a lower pressure and shorter time.

© 2007 WILEY-VCH Verlag GmbH & Co. KGaA, Weinheim

mers exhibits much less rounding than that of the block copolymer, indicating the different rheological behavior between the two kinds of copolymers under the imprinting conditions.

Figure 4 shows the large-area performance of the copolymers, revealing perfect adhesion to the substrate after mold–substrate separation. The mold used was a full four-inch wafer with 100 nm line-width grating features. Figure 4A shows the mold on the left and the imprinted PDMS-*g*-PMA-*co*-PIA surface on the right. Some defects on the original mold, apparent as spots, can be seen replicated in an exact mirror position on the imprinted substrate. Figure 4B is a photograph of blue light diffraction from the periodic gratings imprinted into the PDMS-*g*-PMA-*co*-PIA when the sample is immersed in water. There is some distortion because the light must be viewed through an air/glass/water interface to be visible. Again, the intrinsic mold defect in the center is apparent as an absence of diffracted light in the center of the as-replicated grating field. In each of several successive imprints, there was no apparent gross-delamination of the copolymer, and as a result, no need for solvent rinsing between imprints.

Prior work has shown PMMA to have too strong of an adhesion force to the imprint mold to produce reliable demolding.[6,7] Because of this, large-area performance may be difficult to obtain with the homopolymer. In fact, in our own experiments, the strong adhesion force when imprinting large areas (e.g., four in wafer size) of dense 200 nm period grating structures using PMMA would cause either the mold or the substrate to break during the mold–sample separation. To quantify the advantageous release property given by the PDMS component, the forces required to demold PMMA and PDMS-*g*-PMA-*co*-PIA were compared. The mean copolymer release force was 6.09 N cm^{-2}, while the release force for PMMA was 8.87 N cm^{-2}, which is almost 1.5 times greater.

Etch rates for the copolymers in comparison to various other materials are shown in Table 1. Two T_g values were observed for PS-*b*-PDMS, corresponding to the T_g of the PS ($T_g = 100$ °C) and PDMS blocks ($T_g = -127$ °C), using differential scanning calorimetry (DSC). The presence of two T_gs in the copolymer indicate polymer phase segregation, which is confirmed by using transmission electron microscopy (TEM) analysis (lamellae morphology with a periodicity of 35 nm for a tetrahydrofuran (THF) cast film and 17.4 nm for a microtomed film). The etch rates of the polymers in fluorine plasma are all roughly equivalent. However, there is a large contrast in etch rates in oxygen plasma. PS-*b*-PDMS, with the highest concentration of silicon, shows the lowest O_2 RIE rate, giving it a 13:1 contrast to CHF_3 RIE, and a greater than 100:1 selectivity to PMMA in oxygen plasma. This behavior is expected for PDMS-containing polymers.[16] PDMS-*g*-PMMA and PDMS-*g*-PMA-*co*-PIA, both with lower concentrations of silicon, have correspondingly lower resistances to O_2 RIE. The relatively lower etch rate of PDMS-*g*-PMA-*co*-PIA compared to PDMS-*g*-PMMA at equivalent silicon contents can be attributed to the high C/H ratio of the isobornyl group.

Table 1. Etch rates of copolymer NIL resists in comparison to other materials. Parameters were 20 sccm CHF_3, 20 mTorr (1 Torr = 133.322 Pa), 150 W; 20 sccm O_2, 5 mTorr, 50 W.

Polymer	Si [wt %]	T_g [°C]	CHF_3 [nm min^{-1}]	O_2 [nm min^{-1}]
PS–*b*–PDMS	18.92	–127, 100	13	0.98
PDMS–*g*–PMA-*co*-PIA	7.57	54–64	19	18
PDMS–*g*–PMMA	7.57	105	26	29
PDMS	37.84	–127	26	1.2
PMMA	0	105	20	110

High selectivity to PMMA makes the siloxane copolymer resists ideal materials to be used in bilayer NIL, similar to traditional bilayer photolithography.[18] Figure 5 shows scanning electron microscopy (SEM) images of the original mold features, (A), and the use of the mold to pattern features on the substrate, (B and C). Figure 5A shows the gratings features of the 4 in. mold used in the whole-wafer imprint shown in Figure 4. The substrate was coated with 100 nm of high-molecular-weight PMMA to serve as the undercoating layer, followed by 100 nm of PDMS-*g*-PMA-*co*-PIA resist. The high-molecular-weight PMMA has a slow dissolution rate to minimize intermixing when the NIL resist is applied. However, a small degree of entanglement is expected at the interface, which helps to improve the adhesion. After imprinting there was a thin 30 nm residual layer of resist that was etched in a CHF_3 RIE, followed by a through-etch of the underlayer in 5 mTorr O_2 RIE without breaking vacuum. Such low pressure is necessary to minimize PMMA undercutting at these small feature sizes. The O_2 RIE is applied well beyond the time required to etch through the underlayer to ensure that the exposed substrate surface is thoroughly cleaned by the plasma. In this case, the SiO_2 substrate will not be harmed by the O_2 RIE; this further supports the use of an underlayer rather than etching the resist directly atop the substrate, whereby the residual etch would adversely affect the oxide.

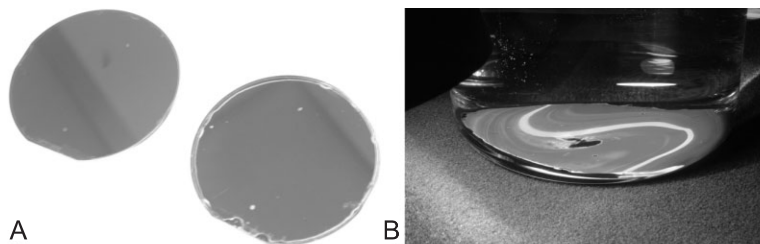

Figure 4. A) A four-inch wafer mold, left, was imprinted into a silicon substrate coated with a PDMS-*g*-PMA-*co*-PIA copolymer, right. B) Strong diffraction of imprinted PDMS-*g*-PMA-*co*-PIA copolymer.

Figure 5B shows the substrate after the O_2 RIE. Resist features at this point consist of a PDMS-*g*-PMA-*co*-PIA copolymer "cap" on top of a PMMA "stem". The vertical side wall of the PMMA is evidence for very little copolymer degradation during the O_2 RIE. Much of the inherent line-edge roughness from the mold, Figure 5A, is mitigated by the residual etch. The lateral width of the resist lines correlates to the narrow width of the bottom of the mold trenches. Such a bilayer resist approach can be used

© 2007 WILEY-VCH Verlag GmbH & Co. KGaA, Weinheim

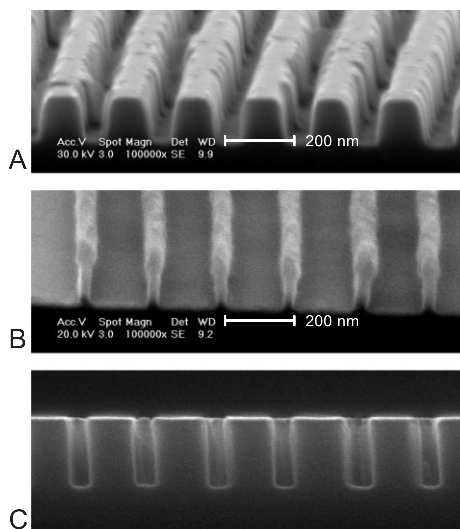

Figure 5. A) 200 nm period mold used to imprint. B) Pattern after the PDMS-*g*-PMA-*co*-PIA residual layer and PMMA undercoating layer were etched. C) Reproduced new mold after all lithography and oxide dry etching.

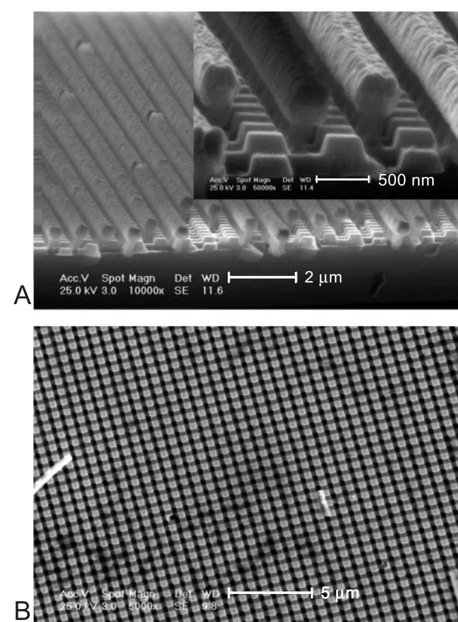

Figure 6. A) Etch resistance of copolymers, in this case PS-*b*-PDMS, allows for complex patterning utilizing an undercoating layer to planarize. B) Two-layer metal grid deposited by two complete NIL steps.

to create very high aspect ratio structures, in this case 3:1. A 20 nm thick nickel layer was evaporated onto the substrate following a 5 nm titanium layer (for adhesion), and then lift-off was performed by dissolving the PMMA underlayer in acetone. The slight undercut profile of the resist in Figure 5B is very advantageous for lift-off processing such as this. The substrate was then treated to a short O_2 RIE to descum any remaining PMMA, and then, without breaking vacuum, a low-pressure O_2 RIE. The Ti–Ni hard mask was then stripped in a 1:1 H_2SO_4 (concentrated)–H_2O_2 (30 %) ("Piranha") solution. The resulting structure is shown in Figure 5C. The hard mask coupled with a low-pressure oxide RIE produces vertical side walls, unlike the angled side walls in the original mold, as seen in Figure 5A. The duty cycle of this new structure corresponds to the duty cycle of the bottoms of the features of the original mold. This process demonstrates the utility of the copolymer NIL resists in nanolithography.

Figure 6 shows the bilayer resist approach used to pattern on top of existing topography. The same process was used as in Figure 5, but this time with PS-*b*-PDMS. A 350 nm line-width mold was used to lift off metal lines. After the first lift-off was complete, the process was repeated in the orthogonal direction. The spin-coated PMMA underlayer served to planarize the nonflat substrate surface. Figure 6A shows the substrate after the second layer of metal was deposited but before lift-off. The grid pattern of the combined metal layers is visible in the cross section, above which is the resist mask covered with metal. Some cracks can be seen on the metal lines on top of the sacrificial resist as a result of the tensile stress as-deposited, but the top is otherwise level, demonstrating the utility of the copolymer resists in bilayer lithography. The resulting metal grid is shown in Figure 6B after the second lift-off step. The square dimensions of the crossed metal lines show that a consistent duty cycle was achieved in both steps.

As previously mentioned, the copolymer resists exhibit some corner rounding, line-edge roughness, and feature-width expansion. Among them, PDMS-*g*-PMA-*co*-PIA has the lowest incidence of roughness and the best corner morphology, and PS-*g*-PDMS exhibits the most roughness and rounded corners. This is possibly due to nonuniform stress relaxation in the bulk resist after pressure and the physical constraint of the mold are released. Further evidence for stress relaxation is the 20 % feature-width expansion of the resist lines. Relaxation of stress involves the rearrangement of polymer chains. Removal of the mold prior to sufficient stress relaxation permits the resist features to alter their morphology. Such behavior has also been observed with homopolymers.[19] To overcome this problem, the internal stress of the resist should be allowed to relax to ambient conditions before molding; however, the corresponding creep rate of plastic polymers is quite long. Nevertheless, such relaxation can be induced in a reasonable time by raising the temperature. In order to test this hypothesis, imprinted copolymer resists are heated at atmospheric pressure and 100 psi to 170 °C for 5 min, without demolding. After cooling again to 40 °C, the samples are demolded. Figure 7 summarizes these results. Figure 7A and C shows imprinted PDMS-*g*-PMA-*co*-PIA and PS-*b*-PDMS, respectively, without annealing. The roughness is so severe in the case of 60 nm PS-*b*-PDMS features that entire void defects occur along the lines. The roughness does not scale with feature size, such that large features (200 nm) do not have this problem, as shown in Figure 7E. There is a great reduction in roughness after annealing, as seen in Figure 7B and D. The 60 nm feature size of the mold is also accurately produced after annealing. PDMS-*g*-PMA-*co*-PIA shows excellent feature reproduction (the mold used is that shown in Fig. 3A), while the void defects in PS-*b*-PDMS lines

© 2007 WILEY-VCH Verlag GmbH & Co. KGaA, Weinheim

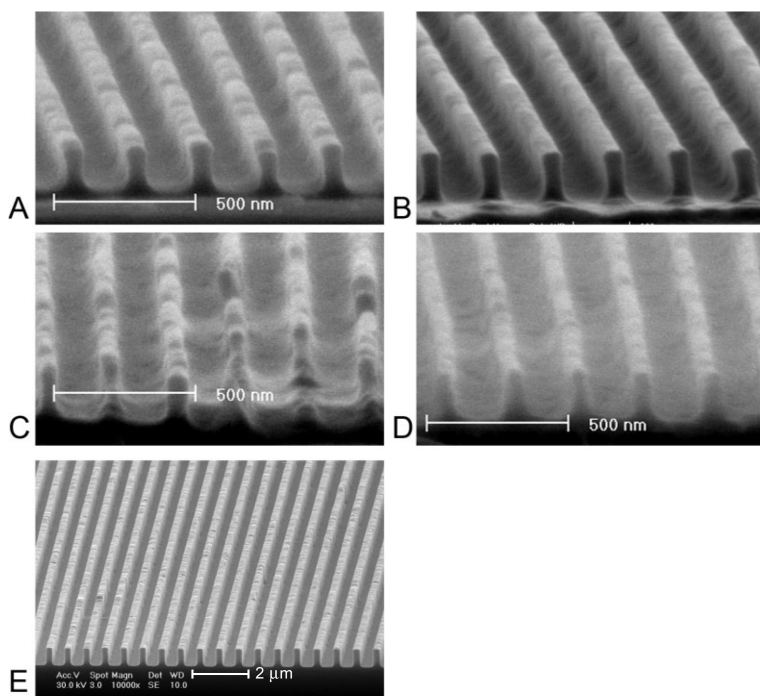

Figure 7. A,C) PDMS-*g*-PMA-*co*-PIA and PS-*b*-PDMS, respectively, after a single imprint cycle, showing roughness and expanded 72 nm features. B,D) Annealing at low pressure reduces roughness and gives 60 nm features. E) PS-*b*-PDMS 200 nm features less prone to roughness.

are also minimized. Although the corner morphology is still better with the annealed PDMS-*g*-PMA-*co*-PIA than with PS-*b*-PDMS, the improvements in both are significant nonetheless.

While samples annealed at 1 atm (1 atm = 101 325 Pa) and 100 psi showed equivalent improvements in pattern morphology, the samples annealed without pressure suffered from dewetting in various places along the mold die. This was because the pressure is necessary to hold the mold and substrate in conformal contact, to overcome surface nonuniformities and particulate contamination. The dewetting problem was eliminated by annealing at 100 psi and taking care not to have particulates in between the mold and the substrates. While the copolymers exhibit nonuniform stress relaxation, unlike homopolymers, such defects can be eliminated by this annealing step.

3. Conclusions

Siloxane organic copolymers have been shown for the first time to be an effective NIL resist material. The dual-surface properties of these copolymers provide superior mold-release performance without delamination—a critical problem facing the NIL area. Furthermore, these copolymers have high silicon content to give them excellent etch resistance, so they can be used as masks to facilitate further pattern transfer to underlying layers. Feature sizes of 50 nm, and possibly below, can be imprinted. Because NIL is a contact process, resists can contaminate the mold. Crosslinked resist systems using UV or thermal curing pose a danger in this regard because of the difficulty when cleaning, so thermoplastic copolymers are safer as any inadvertently contaminating material can be removed easily with solvent.

In principle, any siloxane-based copolymer with higher T_g organic chains should produce a useful NIL resist. In particular, organic components with higher T_g (> 50 °C) are necessary. The resists presented here are single-chain component systems, unlike nonhomogeneous mixtures. Organo-silicone graft copolymers, such as PDMS-*g*-PMA-*co*-PIA and PDMS-*g*-PMMA, are preferred because of their higher degree of homogeneity (less phase segregation) and ease of synthesis.

4. Experimental

Synthesis, Materials and Methods: Toluene and THF were distilled freshly from sodium (3–8 mm sphere)/benzophenone prior to use. Styrene was refluxed over calcium hydride for 4 h and distilled freshly under vacuum prior to use. Anhydrous dimethylformamide (DMF), cyclohexane, *n*-butyl lithium (*n*-BuLi), methacryloxypropyl dimethylchlorosilane were purchased from Aldrich and used directly. All manipulation of air-sensitive materials was performed with the rigorous exclusion of oxygen and moisture in dried Schlenk-type glassware. High-purity argon (Michigan Gas) was used without further purification.

Physical and Analytical Measurements: NMR spectra were recorded on a Varian XL-400 spectrometer. Chemical shifts for ^{1}H, ^{13}C, and ^{29}Si spectra were referenced to an internal solvent resonance and are reported relative to tetramethylsilane. Gel permeation chromatography (GPC) was performed at room temperatures on a Waters 150 CV plus chromatograph equipped with a refractive-index detector. Molecular-weight averages were determined relative to a calibration curve (third order) created using PS standards covering the molecular-weight range of 580–2 300 000 g mol^{-1}. Glass-transition temperatures were measured using DSC, carried out on a DuPont 910 differential scanning calorimeter.

Synthesis of a PDMS–PS Diblock Copolymer: To a three-necked 2 L flask, equipped with a magnetic stir bar and a condenser, under nitrogen, were charged anhydrous cyclohexane (275 mL) and styrene (freshly distilled from CaH_2, 80 g, 0.77 mol). The polymerization was initiated by the introduction of an *n*-BuLi solution (3.2 mL, 1.6 M in hexane), and the solution turned to orange-red immediately. The mixture was stirred at room temperature (RT) for 2.5 h to yield a viscous solution. Next, 100 mL of hexamethylcyclotrisiloxane (D_3) (120 g, 0.54 mol) in anhydrous cyclohexane (350 mL), dried over CaH_2 by refluxing for 2 h, was introduced to the reaction flask. The mixture was then stirred at 60 °C for 1 h; over this time a complete disappearance of the orange-red color was observed. The remaining D_3 cyclohexane solution was added into the reaction flask together with 120 mL of THF. The mixture was refluxed for 6 h to yield an almost clear solution from the originally cloudy one and then cooled down to room temperature. The reaction was terminated with acetic acid (2 mL). The polymer was precipitated by the addition of methanol, collected by filtration, washed with methanol, and dried in a vacuum oven (60–70 °C). Yield: 160.2 g (80.1 %). GPC: number-average molecular weight (M_n) = 45 kg mol^{-1}, M_w/M_n = 1.19 (M_w: weight-average molecular weight). T_g = –127, 100 °C. Weight fraction of each component was approximately 50 %.

Synthesis of Silanol-Capped Polysiloxane Macromonomer: To a 1 L Schlenk flask, equipped with a magnetic stir bar, under nitrogen, were added D_3 (300 g, 1.35 mol), freshly distilled toluene (600 mL), and *n*-BuLi (37.8 mL of 1.6 M in hexane, 60.5 mmol) at room temperature (23 °C). The mixture was stirred for 15 min and followed by the addi-

© 2007 WILEY-VCH Verlag GmbH & Co. KGaA, Weinheim

tion of DMF (32 mL, ca. 10 wt % of D_3) to accelerate the reaction. The reaction was monitored using gas chromatography and stopped at 90 % of D_3 conversion (3.5 h reaction) by the addition of acetic acid (3.685 g, 3.5 mL, 61.4 mmol). The solution was continually stirred for a few hours and then filtrated through a 0.5 µm filter film using a pressure filter (60 psi). After the removal of the volatiles using a rotary pump, the yellowish viscous liquid was washed with acetone/methanol (50:50 volume ratio) to yield a colorless liquid. Yield: 268 g (89.3 %). ^{29}Si NMR (in $CDCl_3$): 7.57 (Bu–$SiMe_2$–), –10.62 (HO–$SiMe_2$–), –21.96 (–$SiMe_2$–); GPC: $M_n = 5119$ g mol^{-1}, $M_w/M_n = 1.05$.

Synthesis of Methacryloxyl-Capped PDMS Macromonomer: To a flamed Schlenk flask under nitrogen were added silanol terminated PDMS macromonomer, Bu$SiMe_2$–$(OSiMe_2)_n$–OH ($M_n = 5119$, $M_w/M_n = 1.05$; 100 g, 19.53 mmol), and triethyl amine (2.56 g, 3.53 mL, 25.4 mmol). The flask was stirred for 2 min and followed by the addition of methacryloxypropyl dimethylchlorosilane (5.61 g, 25.4 mmol) using a syringe. The mixture became cloudy immediately and was stirred for 2 h at RT. The filtration of the mixture through a 0.45 µm pressure filter gave a clear liquid, which yielded a colorless liquid of the title polymer upon the removal of the volatiles under vacuum at 100 °C. Yield: 80 g (80 %). ^{29}Si NMR (in $CDCl_3$): 7.55 (Bu–$SiMe_2$–), 7.35 (–MA–$(CH_2)_3$–$SiMe_2$–), –21.96 (–$SiMe_2$–); GPC: $M_n = 5086$ g mol^{-1}, $M_w/M_n = 1.07$ [20].

Synthesis of PDMS-g-PMMA: To a 500 mL three-necked flask containing a magnetic stirrer bar were charged (methyl methacrylate) (90 g, 0.90 mol), methacryloxyl-capped PDMS macromonomer (10 g, 1.97 mmol), toluene (300 mL), and azobis(isobutyronitrile) (AIBN, 0.1 g) under nitrogen. The mixture was stirred at 65 °C for 18 h. The copolymers were precipitated in methanol, washed with hexanes to remove any unreacted PDMS macromonomer, and dried under reduced pressure. Yield: 85 g (85 %). $T_g = 105$ °C. The PDMS content was approximately 10 wt %.

Synthesis of PDMS-g-PMA-co-PIA: To a 500 mL three-necked flask containing a magnetic stirrer bar were charged isobornyl acrylate (80 g, 0.38 mol), methyl acrylate (10 g, 0.12 mol), methacryloxyl-capped PDMS macromonomer (10 g, 1.97 mmol), toluene (300 mL), and AIBN (0.1 g) under nitrogen. The mixture was stirred at 65 °C for 18 h. The copolymers were precipitated in methanol, washed with hexanes to remove any unreacted PDMS macromonomer, and dried under reduced pressure. Yield: 87 g (87 %). $T_g = 54$–64 °C. PDMS content was approximately 10 wt %.

Sample Preparation: Each polymer was dissolved in PGMEA (MicroChem) and forced through 0.2 µm filters to remove particulates. Solutions were spin-coated onto silicon-wafer substrates and soft-baked at 130 °C. On some samples, a PMMA underlayer ($M_n = 950$ kg mol^{-1}, MicroChem) was spin-coated onto various patterned and unpatterned silicon substrates, baked at 130 °C for 5 min, and coated with a copolymer imprint resist. All samples were hard-baked at 180 °C for 20 min. Although the hard-bake temperature exceeds the T_g of all species, no dewetting problems were observed.

Imprinting Process and Characterization: Imprint molds were patterned thermal oxide on silicon substrates. Some molds were patterned with laser-interference lithography, while others were patterned through a combination of NIL, RIE, or chemical vapor deposition (CVD) processing. Additionally, molds were vapor-coated with tridecafluoro-(1,1,2,2-tetrahydrooctyl)-trichlorosilane (Gelest) at 130 °C in a nitrogen ambient; the surface treatment was annealed for 1 h.

Imprinting was carried out using an NX-2000 (Nanonex) instrument. Samples were vacuum-sealed followed by an imprint at various temperatures, pressures, and times, ranging from 100–170 °C, 200–600 psi, for 30 s–5 min, respectively. Samples were cooled to 40 °C before releasing pressure. In some cases, additional annealing followed at 170 °C and low pressures before demolding.

Release forces were measured with silicon wafer substrates prepared in the aforementioned manner and surfactant-treated grating molds of 700 nm pitch, 50:50 duty cycle, 200 nm feature height, and total area of 4.94 cm^2. After imprinting, each sample was subject to a tensile load normal to the interface plane between mold and substrate using an FDHT force tester (Larson Systems). Peak force, corresponding to the moment before adhesion failure, was recorded at a resolution of ± 0.02 N.

Because of the limited availability of molds, and to maintain experimental consistency, molds were rinsed in solvent prior to each imprint cycle. However, as illustrated, such cleaning does not imply that the resists have delamination issues. Nevertheless, in the event that improper handling leads to contamination of the mold by these copolymer resists, they can be readily dissolved in appropriate solvents, such as PGMEA or acetone, since these PDMS copolymers are amorphous materials. The easy cleaning feature of these thermoplastic resists offers a processing advantage over crosslinking (or "curing") resists [21], which are typically very difficult to clean or remove from the mold. Crosslinked polymers generally must be plasma-etched in the event that it contaminates the valuable imprint mold, potentially jeopardizing the pattern fidelity.

To characterize the etch behavior of the copolymers, a capacitively coupled RIE instrument was used. Typical flow gas rates were 20 sccm with a chamber pressure ranging from 5 to 20 mTorr, and power from 50 to 150 W. RIE was used to etch the polymer residual, undercoating, and SiO_2. Metal lift-off was performed by evaporating layers of Ti and Ni onto substrates, and dissolving the PMMA undercoating in acetone. Thicknesses were measured using ellipsometry. Imprinted structure morphology was inspected with a scanning electron microscope.

Received: March 21, 2006
Revised: June 22, 2006
Published online: November 24, 2006

[1] S. Y. Chou, P. R. Krauss, P. J. Renstrom, *Appl. Phys. Lett.* **1995**, *67*, 3114.
[2] S. Y. Chou, P. R. Krauss, P. J. Renstrom, *Science* **1996**, *272*, 87.
[3] S. Y. Chou, P. R. Krauss, W. Zhang, L. J. Guo, L. Zhuang, *J. Vac. Sci. Technol. B* **1997**, *15*, 2897.
[4] L. J. Guo, *J. Phys. D: Appl. Phys.* **2004**, *37*, R123.
[5] *Technol. Rev.* **2003**, *106*, 36.
[6] Y. Chen, D. Macintyre, E. Boyd, D. Moran, I. Thayne, S. Thoms, *J. Vac. Sci. Technol. B* **2002**, *20*, 2887.
[7] Y. Hirai, S. Yoshida, N. Takagi, *J. Vac. Sci. Technol. B* **2003**, *21*, 2765.
[8] M. Beck, M. Graczyk, I. Maximov, E. L. Sarwe, T. G. I. Ling, M. Keil, L. Montelius, *Microelectron. Eng.* **2002**, *61–62*, 441.
[9] J. C. Saam, D. J. Gordon, S. Lindsey, *Macromolecules* **1970**, *3*, 1.
[10] T. Pakula, G. Floudas, in *Block Copolymers* (Eds: F. J. Balta Calleja, Z. Roslaniec), Marcel Dekker, New York **2000**, Ch. 6.
[11] N. Hadjichristidis, S. Pispas, G. Floudas, *Block Copolymers*, Wiley, New York **2003**.
[12] I. W. Hamley, *The Physics of Block Copolymers*, Oxford University Press, Oxford **1998**.
[13] P. F. Fu, *Polym. Prepr. (Am. Chem. Soc., Div. Polym. Chem.)* **2003**, *44*, 788.
[14] P. F. Fu, M. K. Tomalia, *Macromolecules* **2004**, *37*, 267.
[15] X. Chen, J. A. Gardella, Jr., P. L. Kumler, *Macromolecules* **1992**, *25*, 6631.
[16] N. J. Chou, C. H. Tang, J. Paraszczak, E. Babich, *Appl. Phys. Lett.* **1985**, *46*, 31.
[17] H. Schulz, H. C. Scheer, T. Hoffman, C. M. S. Torres, K. Pfeiffer, G. Gleidiessel, G. Grutzner, C. Cardinaud, F. Gaboriau, M. C. Peignon, J. Ahopelto, B. Heidari, *J. Vac. Sci. Technol. B* **2000**, *18*, 1861.
[18] D. C. Hofer, R. D. Miller, C. G. Willson, *Proc. Soc. Photo-Opt. Instrum. Eng.* **1984**, *469*, 16.
[19] C. Martin, L. Ressier, J. P. Peyrade, *Phys. E* **2003**, *17*, 523.
[20] S. D. Smith, J. M. DeSimone, H. Huang, G. York, D. W. Dwight, G. L. Wilkes, J. E. McGrath, *Macromolecules* **1992**, *25*, 2575.
[21] M. Colburn, S. Johnson, M. Stewart, S. Damle, T. Bailey, B. Choi, M. Wedlake, T. Michaelson, S. V. Sreenivasan, J. G. Ekerdt, C. G. Willson, *Proc. SPIE-Int. Soc. Opt. Eng.* **1999**, *3676*, 379.

© 2007 WILEY-VCH Verlag GmbH & Co. KGaA, Weinheim